PAPER

Bound states in the continuum in open spherical resonator

IOP Publishing Physica Scripta
Phys. Scr. 95 (2020) 085002 (7pp) https://doi.org/10.1088/1402-4896/ab99fb

Bound states in the continuum in open spherical resonator

A S Pilipchuk, A A Pilipchuk and A F Sadreev

Kirensky Institute of Physics, Federal Research Center KSC SB RAS, 660036 Krasnoyarsk, Russia

E-mail: artem-s-pilipchuk@iph.krasn.ru

Received 25 February 2020, revised 27 May 2020
Accepted for publication 5 June 2020
Published 16 June 2020

Abstract

We consider the bound states in the continuum (BICs) or embedded trapped modes in an open spherical acoustic resonator. The eigenfrequencies of closed resonator are $2l + 1$-fold degenerated, where l is the orbital index. An attachment of two cylindrical waveguides lifts this degeneracy and transforms the eigenfrequencies into resonances whose real parts depend on the position of the waveguides. When the waveguides are angled by $\theta \neq \pi$, variation over that angle gives rise to avoided crossings of resonant modes with different l to result in the Friedrich-Wintgen BICs. For $\theta = \pi$ there might be only the symmetry protected BICs. When three waveguides are connected to the spherical resonator the Friedrich-Wintgen BICs occur due to the avoided crossings of resonant modes with the same l but different azimuthal indices $-l \leqslant m \leqslant l$.

Keywords: bound states in the continuum, effective non-Hermitian Hamiltonian, acoustic resonator, trapped modes

(Some figures may appear in colour only in the online journal)

1. Introduction

Bound states in the continuum (BIC) also known as embedded trapped modes are localized solutions which correspond to discrete eigenvalues coexisting with extended modes of continuous spectrum in resonator-waveguide configurations. The existence of trapped solutions residing in the continuum was first reported by von Neumann and Wigner [1] at the dawn of quantum mechanics. In the field of fluid mechanics, Parker [2, 3] is credited to be the first to encounter resonances of pure acoustic nature in the air flow over a cascade of flat parallel plates. Nowadays, the BICs are known to exist in various waveguide structures ranging from quantum wires [4–8], acoustic waveguides [9–13], and photonic crystals [14–16]. The BICs are of immense interest, specifically, in photonics due to experimental opportunity to confine light in optical microcavities despite the fact that outgoing waves are allowed in the surrounding radiation continuum [16–19]. At the same time, in aerodynamics, trapped and nearly trapped modes are known to cause severe vibrations and noise problems in gas and steam pipelines [20, 21].

The generic mechanism of full destructive interference for the BICs was proposed by Friedrich and Wintgen in 1985 [22]. When two resonances avoid each other as a function of a certain continuous parameter, the interaction between them through the continuum may cause the width of one of hybridized resonances to vanish exactly. An equivalent explication of BICs is that under variation of the system parameter the eigenmodes ψ_1, ψ_2 of the same symmetry become degenerate. Then, the coupling of the superposed state $a_1\psi_1 + a_2\psi_2$ with the continuum can be cancelled by a proper choice of the superposition coefficients a_1 and a_2 [7]. This principle was later explored in open integrable rectangular and cylindrical resonators where the BIC occurs in the vicinity of the degeneracy point for variation of aspect ratio of the resonators [12, 13].

The eigenmodes of closed spherical resonator are $2l + 1$-fold degenerated spherical functions, where l is the orbital index. The only parameter to vary is the resonator radius which only scales the resonator eigenvalues by the factor $1/R^2$. Therefore it seems that the FW mechanism for the BICs due to an avoided crossing can not be applied here. Let us open the spherical resonator by attaching of two cylindrical waveguides, which lifts the degeneracy. The continua of the waveguides in the form of propagating Bessel modes transform the discrete eigenfrequencies of the closed

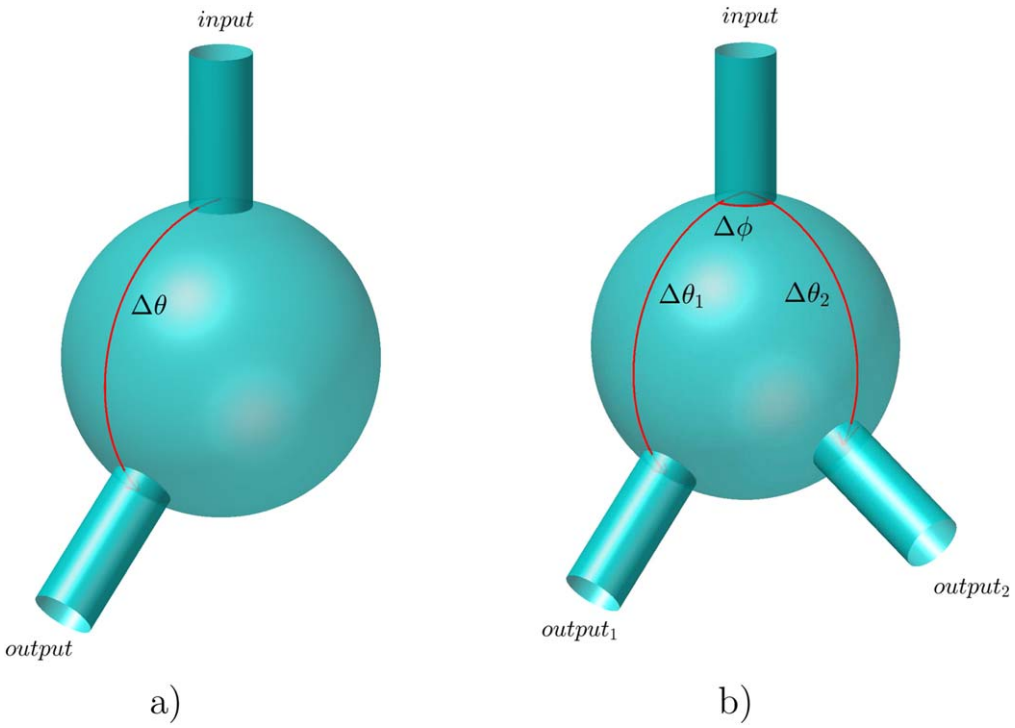

Figure 1. Spherical resonator of radius R with two (a) and three (b) asymmetrically attached cylindrical waveguides of the same radii r_w.

resonator into the complex resonant frequencies the positions of which depend on overlapping of the spherical functions with the Bessel modes. In turn, if the waveguides are angled by $\theta \neq \pi$, variation over that angle can give rise to avoided crossings of resonant modes with different l to result in the Friedrich-Wintgen BICs. The paper was inspired by a similar case of the cylindrical resonator opened by non-coaxial attachment of two waveguides. It was shown that a rotation of one of the waveguides around the resonator axis gives rise to numerous events of avoided crossing of open system resonances with different azimuthal indices m, and respectively to the FW BICs [23].

Furthermore, connection of three cylindrical waveguides to the spherical resonator opens a way for the full destructive interference of the resonator eigenfunctions with the same indices l but different azimuthal indices $-l \leqslant m \leqslant l$. For this purpose one of the waveguides is connected to the pole of the spherical resonator, the second one is deflected from the pole by the angle $\Delta\theta_1$ and the third one is shifted by the two angles $\Delta\theta_2$ and $\Delta\phi$ as schematically shown in the figure 1(b). Such a connection makes it possible to use two variation parameters —the polar angle $\Delta\theta$ and the azimuthal angle $\Delta\phi$ simultaneously.

2. Coupled mode theory

We use the acoustic coupled mode theory (CMT) which is efficient both for calculating the transmittance through acoustical waveguide-resonator systems and for searching of BICs [24]. It is easy to find the solution of the Helmholtz equation in spherical coordinates:

$$\Psi_{lmn} = \Psi_{ln}(r)\,Y_{lm}(\theta,\,\phi)$$

$$\Psi_n(r) = \frac{1}{R^{3/2}}\sqrt{\frac{2}{\kappa_{l+1/2,n}^2 - n(n+1)}} \times \frac{\kappa_{l+1/2,n}}{J_{l+1/2}(\kappa_{l+1/2,n})} J_{l+1/2}\left(\frac{\kappa_{l+1/2,n} r}{R}\right)$$

$$Y_{lm}(\theta,\,\phi) = \sqrt{\frac{(2l+1)(l-m)!}{4\pi(l+m)!}}\,P_{lm}(\cos\theta)\exp(\mathrm{i}m\phi) \quad (1)$$

where r, θ, ϕ are the spherical coordinates, R is the spherical resonator radius, Y_{lm} are the spherical harmonics, $P_{lm}(\cos\theta)$ are the associated Legendre polynomials, $J_{l+1/2}$ are the Bessel functions, $\kappa_{l+1/2,n}$ are the roots of the equation $dJ_{l+1/2,n}(\kappa_{l+1/2,n} r/R)/\mathrm{d}r|_{r\,=\,R} = 0$. Respective eigenfrequencies of the closed spherical resonator are given:

$$\omega_{nl}^2 = \kappa_{l+1/2,n}^2 \big/ R^2. \quad (2)$$

All the quantities are dimensionless and expressed in terms of the cylindrical waveguides radius r_w. The dimensionless frequency ω is expressed through the dimensional one $\tilde{\omega}$ as follows: $\omega = \tilde{\omega} r_w / s$, where s is the sound velocity.

The eigenfunctions of the cylindrical waveguides are:

$$\psi_{pq}^{(C)}(\rho,\,\alpha,\,z) = \psi_{pq}^{(C)}(\rho)\frac{1}{\sqrt{2\pi k_{pq}^{(C)}}}\exp(\mathrm{i}p\alpha + \mathrm{i}k_{pq}^{(C)} z),$$

$$\psi_{pq}^{(C)}(\rho) = \begin{cases} \dfrac{\sqrt{2}}{r_C J_0(\mu_{0q})} J_0\left(\dfrac{\mu_{0q}\rho}{r_C}\right), \; p = 0, \\ \sqrt{\dfrac{2}{\mu_{pq}^2 - p^2}}\,\dfrac{\mu_{pq}}{r_C J_p(\mu_{pq})} J_p\left(\dfrac{\mu_{pq}\rho}{r_C}\right), \; p = 1,\,2,\,3,\ldots, \end{cases} \quad (3)$$

where ρ, α are the polar coordinates in the $x0y$-plane in the

waveguides reference system, $Jp(x)$ are the cylindrical Bessel functions of the first kind, μ_{pq} is the q-th root of equation $dJ_p(\mu_{pq}\rho)/\mathrm{d}\rho|_{\rho=r_C} = 0$ imposed by the Neumann boundary condition on the walls of sound hard cylindrical waveguide, C enumerates input and output waveguides, $k_{pq}^{(C)}$ is the wave number:

$$k_{pq}^{(C)} = \sqrt{\omega^2 - \mu_{pq}^2/r_C^2}, \tag{4}$$

The CMT starts with a formulation of the non-Hermitian effective Hamiltonian [23, 24]

$$H_{\mathrm{eff}} = H_{\mathrm{B}} - \mathrm{i}\sum_{C}\sum_{pq} k_{pq}^{(C)} W_{pq}^{(C)} W_{pq}^{(C)\dagger}, \tag{5}$$

where H_{B} is the Hamiltonian of the closed resonator whose eigenmodes and eigenfrequencies are given by equations (1) and (2) and the coupling matrices of the resonator eigenmodes with the propagating modes are determined by the overlapping integrals [23, 24]:

$$W_{lmn,pq} = \Psi_{ln}(r = R)\int_0^{2\pi} \mathrm{d}\phi \times \int_0^1 \rho \mathrm{d}\rho \psi_{pq}(\rho, \phi) Y_{lm}(\theta(\rho, \phi), \phi) \tag{6}$$

where ρ is the radius in the cylindrical reference frame, $\phi = \alpha$ is the azimuthal angle, θ is the polar angle in the spherical reference frame. To perform this integration one has to express the spherical coordinates in terms of the cylindrical ones which could be done by a simple mathematical transformation. Rigorously, the integration is carried out over an interface between the sphere of the radius R and cylindrical waveguides with the radius $r_w = 1$. For $R \gg 1$ the circular interface can be approximated by the flat interface.

In order to calculate the coupling matrix elements for asymmetrically connected waveguides we take that each waveguide is attached to the pole of the spherical resonator but rotate the resonator eigenfunctions by using the Wigner D-matrix:

$$D_{mk}^{l}(\alpha, \beta, \gamma) = \exp(-\mathrm{i}k\alpha) d_{mk}^{l}(\beta) \exp(-\mathrm{i}m\gamma), \tag{7}$$

where α, β, γ are the Euler's angles and $d_{mk}^{l}(\beta)$ is the small Wigner matrix:

$$d_{mk}^{l} = \sqrt{\frac{(l-m)!(l+m)!}{(l-k)!(l+k)!}} \sum_{s=\max(0,k-m)}^{\min(l-m,l+k)} (-1)^{m-k+s} \binom{l+k}{s}\binom{l-k}{m-k+s} \cos^{2l-m+k-2s}\left(\frac{\beta}{2}\right) \sin^{m-k+2s}\left(\frac{\beta}{2}\right) \tag{8}$$

Then the rotated spherical harmonics can be expressed through the non-rotated ones as follows:

$$\tilde{Y}_m^l(\theta, \phi) = \exp(-\mathrm{i}m\gamma) \sum_{k=-l}^{l} \exp(-\mathrm{i}k\alpha) d_{mk}^{l}(\beta) Y_k^l(\theta', \alpha') \tag{9}$$

As a result the coupling matrix elements of the resonator with asymmetrically connected waveguides are

$$\tilde{W}_{lmn,pq} = \exp(-\mathrm{i}m\gamma) \sum_{k=-l}^{l} \exp(-\mathrm{i}k\alpha) d_{mk}^{l} W_{lkn,pq} \tag{10}$$

The transmission coefficients from the channel pq of the waveguide (C) to the channel $p'q'$ of the waveguide (C') are given by the following equations [23, 24]:

$$t_{pq;p'q'}^{(CC')} = 2\mathrm{i}\sqrt{k_{pq}^{(C)} k_{p'q'}^{(C')}} \sum_{lmn}\sum_{l'm'n'} W_{lmn;pq}^{(C)} \frac{1}{\omega^2 - H_{eff}} W_{l'm'n';p'q'}^{(C')*}, \tag{11}$$

3. Two waveguides

Let the first waveguide be attached to the resonator at the pole and the second one be attached at the angle $\Delta\theta$ as shown in the figure 1(a). Such an attachment of the waveguides lifts the $2l + 1$-fold degeneracy of the closed spherical resonator eigenvalues. Indeed, one can see from figure 2 that rotation of the second waveguide relative to the first waveguide splits resonances with the angle $\Delta\theta$ where the positions of the resonances are given by real parts of the complex eigenvalues of the non Hermitian Hamiltonian [24, 25]. However it is more remarkable that the rotation gives rise to avoided crossings of resonances with different orbital indices l and respectively to the FW BIC which is marked by large open circle.

Figure 2 shows the transmittance versus the frequency of the wave injected into the first waveguide and the angle $\Delta\theta$. One can see that the narrow transmission peaks follow to the resonant frequencies marked by small open circles. Small resonant widths are the result of that the three dimensional resonator is weakly coupled with the waveguides if the radius of the resonator substantially exceeds the waveguides radii ($R \gg r_w$) [23]. Indeed, the normalization coefficients of the spherical resonator eigenmodes (3) are proportional to $\frac{1}{R^{3/2}}$. The coupling matrix elements (6) preserve this factor. Then the resonant widths given by squared coupling matrix elements are proportional to $\frac{1}{R^3}$ while the distances between the eigenfrequencies of the closed resonator are proportional to $\frac{1}{R^2}$.

Wave transmission through resonators specified by transmission peaks is related to the resonant states with complex eigenfrequencies of the effective Hamiltonian [24, 25]. In the one-dimensional case the neighboring resonances differ by symmetry relative to inversion of one-dimensional axis, therefore the transmission zeros are absent [26, 27]. In other words, there is no destructive interference of resonances in the one-dimensional wave transmission except, however, the case of vector field transmission [28, 29]. In the two- and three-dimensional cases this rule for symmetry of neighboring resonances is not valid to give rise to destructive interference of them and therefore to zeros of transmission [26, 27]. A frequency dependence of the transmittance takes asymmetric form similar to Fano resonance which is a result of destructive interference of pathways [30, 31]. Therefore the Friedrich-Wintgen BICs [22] resulted by avoided crossing of resonances respectively are accompanied by convergence of the transmission peak and transmission zero to result in the

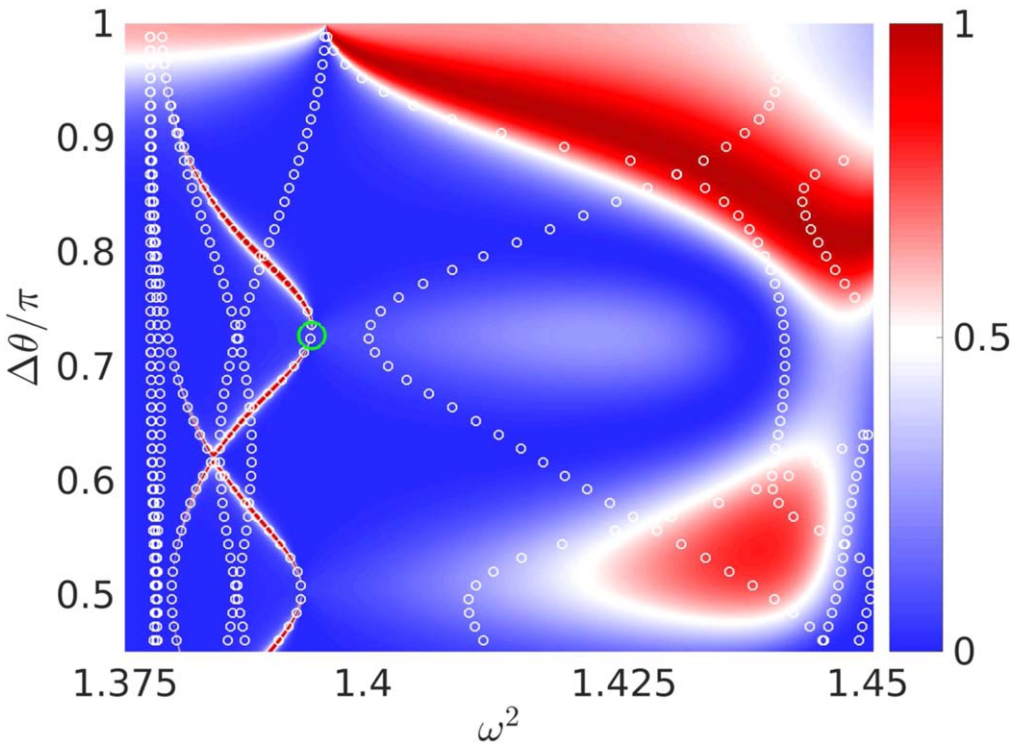

Figure 2. Transmittance of the spherical resonator versus the frequency of injected wave and displacement angle of the second waveguide. Small open circles mark the real parts of complex open spherical resonator eigenfrequencies versus the second waveguide displacement angle. Large open circle indicates the BIC point where the collapse of Fano resonance occurs.

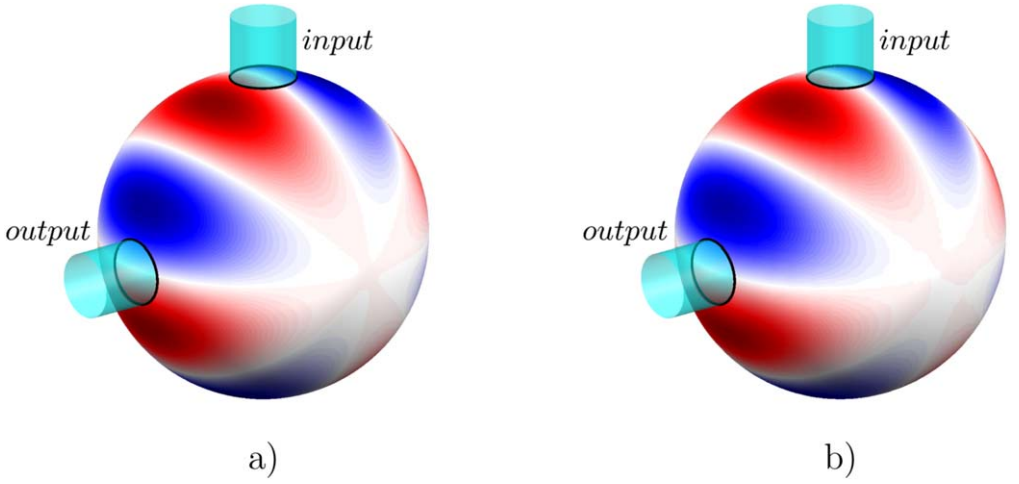

Figure 3. (a) The pressure field of SP BIC on the surface of spherical resonator with $\omega = 1.3748$ and $\Delta\theta = 0.5048\pi$. (b) The rotated by the same angle spherical harmonic with $l = 4$, $m = 1$.

collapse of Fano resonance, which is a signature of the BIC [5, 7].

Figure 2 shows several points of the BIC at certain frequencies ω and rotation angles $\Delta\theta$ which also can be found by vanishing of imaginary parts of the complex eigenvalues of the non Hermitian effective Hamiltonian. The major part of the BICs in the case of two waveguides are symmetry protected (SP) and are simply the rotated eigenfunctions of the closed resonator orthogonal to the propagating waveguide mode. Figure 3(a) shows the pressure field on the surface of the resonator for one of the SP BICs. One can see that this SP BIC coincides with the resonator eigenmode shown in figure 3(b) which depicts a spherical harmonic with indices $l = 4$, $m = 1$ rotated using the Wigner D-matrix.

Moreover as seen from figure 2 there is also a FW BIC at the point $\Delta\theta = 0.727\pi$, $\omega = 1.378$ marked by the large open circle. Figure 4(a) shows the wave function (the pressure field) of this BIC on the resonator surface. One can see from nodal lines ($\Psi_{BIC} = 0$) that the coupling of this state with the propagating mode of the waveguides with indices $p = 0$, $q = 1$ equals zero. The modal expansion of this FW BIC is shown in figure 4(b). The resonator eigenmodes with different

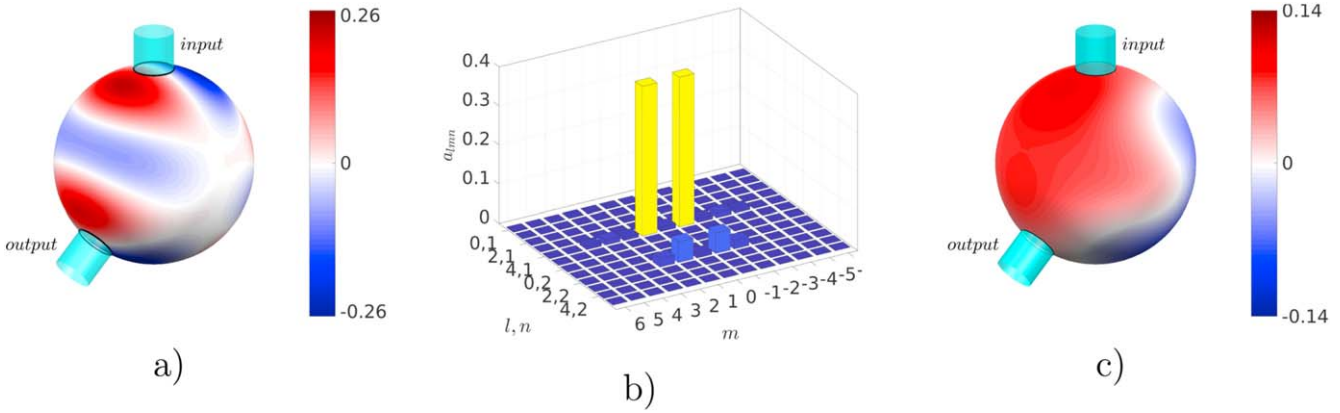

Figure 4. (a) The pressure field of of the FW BIC on the surface of spherical resonator with $\omega = 1.3937$ and $\Delta\theta = 0.727\pi$. The circles indicate areas where the waveguides are connected. (b) The modal decomposition of the BIC. (c) Superradiant (low-Q) mode which exists along with the BIC function.

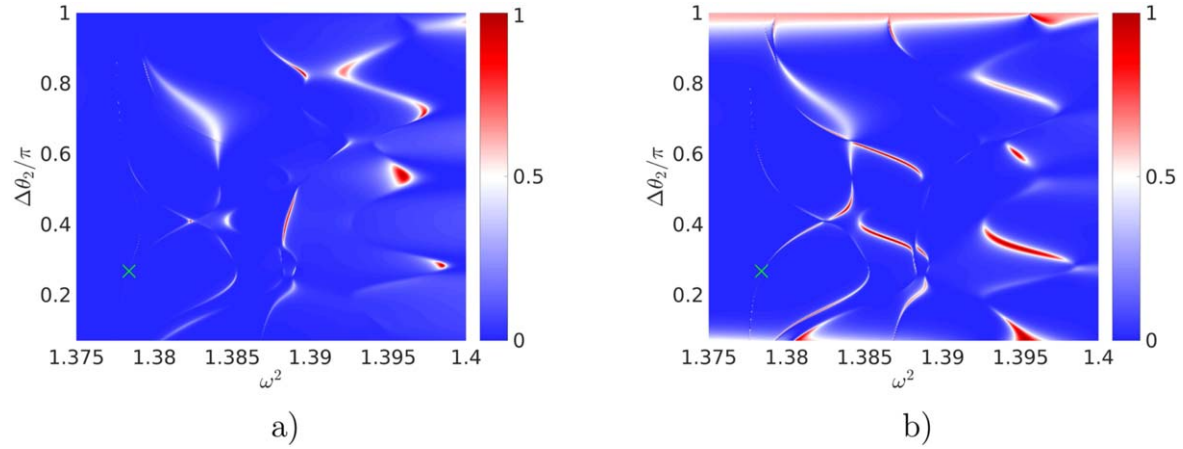

Figure 5. Transmittance of the spherical resonator versus frequency and the displacement angle $\Delta\theta_2$ of the third waveguide for $\Delta\phi = \pi/4$ (a) between waveguides *input* and *output*$_2$; (b) between waveguides *input* and *output*$_1$. The displacement angle of the second waveguide is $\Delta\theta_1 = 3\pi/4$. The cross designates the position of BIC.

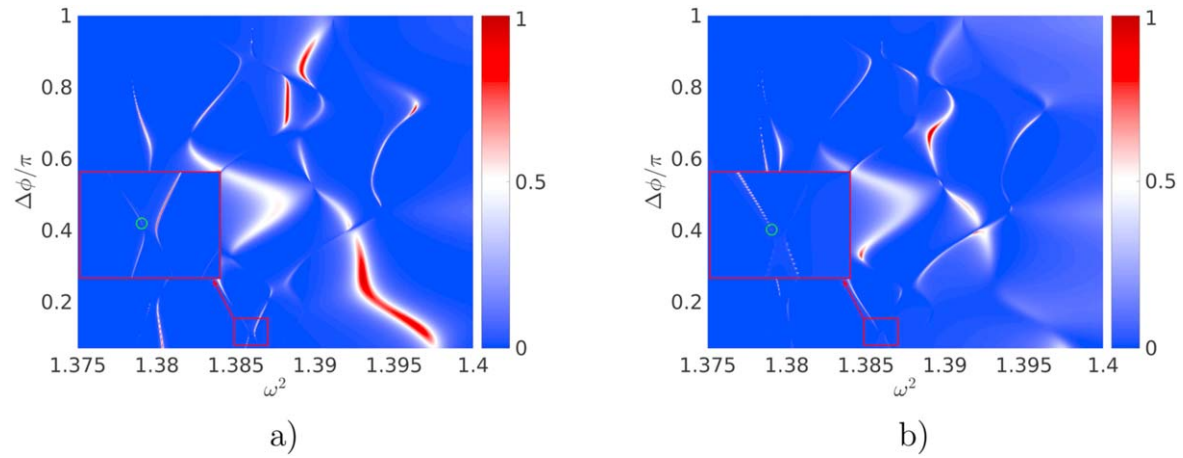

Figure 6. Transmittance of the spherical resonator versus frequency and the displacement angle $\Delta\phi$ of the third waveguide for $\Delta\theta_2 = \sqrt{2}$ (a) between waveguides *input* and *output*$_2$; (b) between waveguides *input* and *output*$_1$. The displacement angle of the second waveguide is $\Delta\theta_1 = \sqrt{5}$.

l contribute into the BIC in full agreement with figure 2. Thus, the FW BIC is the result of full destructive interference of resonant modes with different orbital indices, despite the fact

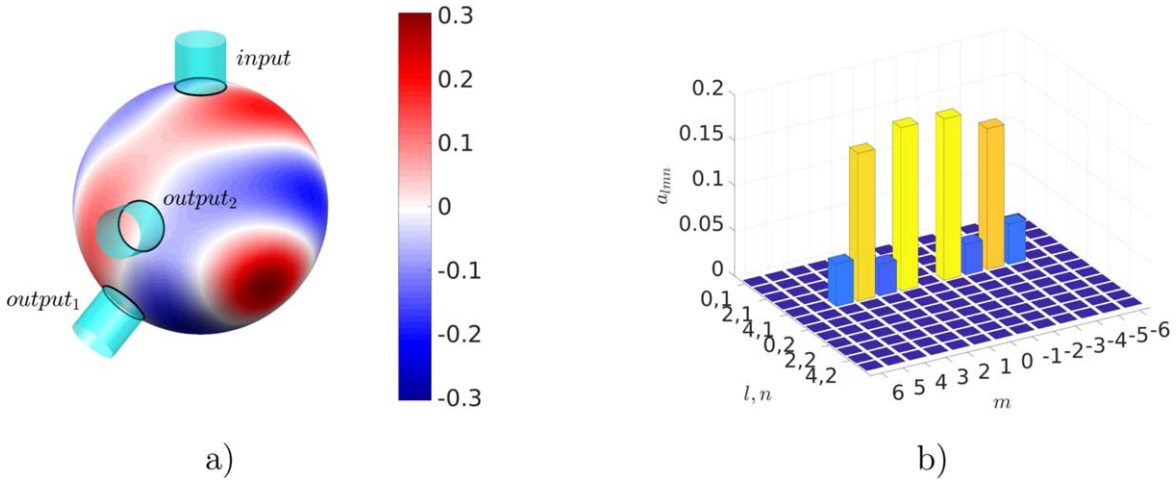

Figure 7. (a) The pressure field on the surface of spherical resonator at the BIC point with $\omega = 1.38575$, $\Delta\theta_1 = \sqrt{5}$, $\Delta\theta_2 = \sqrt{2}$ and $\Delta\phi = 0.1222\pi$. The circles indicate areas where the waveguides are connected. (b) The modal decomposition of the BIC.

that the eigenmodes of the closed spherical resonator have different frequencies (2). Note that the BIC mode is always complemented by the superradiant (low-Q) mode, that is shown in figure 4(c). This mode has the maximal coupling with the continuum [32].

4. Three waveguides

Although the position of the second waveguide relative to the first one at the pole of a sphere is given by the two angles in general, only the polar angle $\Delta\phi$ is physically relevant for resonances and, in particular, for BICs. The introduction of the third waveguide as shown in figure 1(b) cardinally changes effects of the continua onto the resonances because of three relevant angles, two polar angles $\Delta\theta_1$, $\Delta\theta_2$ and one azimuthal angle $\Delta\phi$.

Figures 5 and 6 show the transmittance versus the frequency of the injected wave and rotation angles $\Delta\theta_2$ and $\Delta\phi$, thus demonstrating evident importance of mutual orientations of all the waveguides. The regions in which avoid crossing phenomenon occurs, as well as the collapse of the Fano resonance, are highlighted by frames. The circle in the figure 6 marks the position of the FW BIC whose surface pressure is shown in the figure 7(a). It is interesting that in this case the resonator eigenlevels with the same orbital indices l interfere, which is confirmed by figure 7(b), where the modal decomposition of this BIC is shown.

5. Conclusion

The well-developed strategy for FW BICs based on full destructive interference of two resonances for avoided crossing in open resonators implies that waveguides support only one continuum. In our case of cylindrical waveguides the continua are given by propagating channels enumerated by indices p, q according to equation (4). By proper choice of frequency one can open these channels one by one. When the frequency is below the second cutoff only the first channel $p = 0$, $q = 1$ is opened while other channels of waveguide are evanescent. They have imaginary wave vectors k_{pq} and contribute into the effective non hermitian Hamiltonian (5) by means of real parts that modifies the Hamiltonian of the resonator and respectively shifts its eigenfrequencies [23]. As a result, the BIC points do not coincide exactly with the degeneracy points of the closed resonator [7]. Also the evanescent modes of waveguides give rise to exponential decay of the BIC modes into the waveguides in the form $\exp(-|k_{pq}|z)$ [33]. The above said was demonstrated in rectangular and cylindrical waveguides.

For the first time the nontrivial role of the waveguides evanescent modes was demonstrated in open cylindrical resonators when cylindrical waveguides were shifted relative to each other by some angle $\Delta\phi$ [23]. Respectively the shifted eigenfrequencies of the resonator become dependent on this angle and numerous events of avoided crossings were observed for rotation over $\Delta\phi$ with formation of FW BICs in addition to the FW BICs formed by degeneracy of the closed cylindrical resonator eigenfrequencies for the variation of its length. The spherical resonator is unique because there is no accidental degeneracy for the variation of its radius. But similar to the case of non-axisymmetric cylindrical waveguide [23] attachment of at least two cylindrical waveguides to the spherical resonator asymmetrically lifts the $2l + 1$-fold degeneracy of the eigenfrequencies and what is more important gives rise to avoided crossing of these splitted eigenfrequencies from different multiplets. Indeed, in the present paper we report the FW BICs in the spherical acoustic resonator with two and three connected cylindrical waveguides.

Acknowledgments

The reported study was supported by Russian Foundation for Basic Research (RFBR) according to the research project 18-32-00234.

ORCID iDs

A S Pilipchuk https://orcid.org/0000-0002-8596-1331
A F Sadreev https://orcid.org/0000-0002-8690-0100

References

[1] von Neumann J and Wigner E 1929 Über merkwürdige diskrete Eigenwerte *Phys. Z.* **30** 465–7
[2] Parker R 1966 Resonance effects in wake shedding from parallel plates: some experimental observations *J. Sound Vib.* **4** 62–72
[3] Parker R 1967 Resonance effects in wake shedding from parallel plates: calculation of resonant frequencies *J. Sound Vib.* **5** 330–43
[4] Shahbazyan T V and Raikh M E 1994 Two-channel resonant tunneling *Phys. Rev.* B **49** 17123–9
[5] Kim C S, Satanin A M, Joe Y S and Cosby R M 1999 Resonant tunneling in a quantum waveguide: effect of a finite-size attractive impurity *Phys. Rev.* B **60** 10962
[6] Olendski O and Mikhailovska L 2002 Bound-state evolution in curved waveguides and quantum wires *Phys. Rev.* **66** 035331 B
[7] Sadreev A F, Bulgakov E N and Rotter I 2006 Bound states in the continuum in open quantum billiards with a variable shape *Phys. Rev.* B **73** 235342
[8] Cattapan G and Lotti P 2007 Fano resonances in stubbed quantum waveguides with impurities *Eur. Phys. J.* B **60** 51–60
[9] Linton C M and McIver P 2007 Embedded trapped modes in water waves and acoustics *Wave Motion* **45** 16–29
[10] Duan Y, Koch W, Linton C M and McIver M 2007 Complex resonances and trapped modes in ducted domains *J. Fluid Mech.* **571** 119–47
[11] Hein S and Koch W 2008 Acoustic resonances and trapped modes in pipes and tunnels *J. Fluid Mech.* **605** 401–28
[12] Hein S, Koch W and Nannen L 2012 Trapped modes and fano resonances in two-dimensional acoustical duct–cavity systems *J. Fluid Mech.* **692** 257–87
[13] Lyapina A A, Maksimov D N, Pilipchuk A S and Sadreev A F 2015 Bound states in the continuum in open acoustic resonators *J. Fluid Mech.* **780** 370–87
[14] Bulgakov E N and Sadreev A F 2008 Bound states in the continuum in photonic waveguides inspired by defects *Phys. Rev.* B **78** 075105
[15] Marinica D C, Borisov A G and Shabanov S V 2008 Bound states in the continuum in photonics *Phys. Rev. Lett.* **100** 183902
[16] Hsu C W, Zhen B, Lee J, Chua S-L, Johnson S G, Joannopoulos J D and Soljačić M 2013 Observation of trapped light within the radiation continuum *Nature* **499** 188–91
[17] Plotnik Y, Peleg O, Dreisow F, Heinrich M, Nolte S, Szameit A and Segev M 2011 Experimental observation of optical bound states in the continuum *Phys. Rev. Lett.* **107** 28–31
[18] Weimann S, Yi X, Keil R, Miroshnichenko A E, Tünnermann A, Nolte S, Sukhorukov A A, Szameit A and Kivshar Y S 2013 Compact surface fano states embedded in the continuum of waveguide arrays *Phys. Rev. Lett.* **111** 240403
[19] Bulgakov E N and Sadreev A F 2014 Bloch bound states in the radiation continuum in a periodic array of dielectric rods *Phys. Rev.* A **90** 053801
[20] Aly K and Ziada S 2016 Review of flow-excited resonance of acoustic trapped modes in ducted shallow cavities *J. Pressure Vessel Techn.* **138** 040803
[21] Ziada S, Bolduc M and Lafon P 2017 Flow-excited resonance of diametral acoustic modes in ducted rectangular cavities *AIAA J.* **55** 3817–30
[22] Friedrich H and Wintgen D 1985 Interfering resonances and bound states in the continuum *Phys. Rev.* A **32** 3231–42
[23] Lyapina A A, Pilipchuk A S and Sadreev A F 2018 Trapped modes in a non-axisymmetric cylindrical waveguide *J. Sound Vib.* **421** 48–60
[24] Maksimov D N, Sadreev A F, Lyapina A L and Pilipchuk A S 2015 Coupled mode theory for acoustic resonators *Wave Motion* **56** 52–66
[25] Rotter I 1991 A continuum shell model for the open quantum mechanical nuclear system *Rep. Prog. Phys.* **54** 635
[26] Lee H-W 1999 Generic transmission zeros and in-phase resonances in time-reversal symmetric single channel transport *Phys. Rev. Lett.* **82** 2358
[27] Sadreev A F and Rotter I 2003 S-matrix theory for transmission through billiards in tight-binding approach *J. Phys.* A **36** 11413–33
[28] Quotane I *et al* 2018 Trapped-mode-induced fano resonance and acoustical transparency in a one-dimensional solid-fluid phononic crystal *Phys. Rev.* B **97** 024304
[29] Pankin P S, Wu B-R, Yang J-H, Chen K-P, Timofeev I V and Sadreev A F 2020 One-dimensional photonic bound states in the continuum *Communications Physics* **3** 1–8
[30] Fano U 1961 Effects of configuration interaction on intensities and phase shifts *Phys. Rev.* **124** 1866
[31] Rotter S, Libisch F, Burgdörfer J, Kuhl U and Stöckmann H-J 2004 Tunable fano resonances in transport through microwave billiards *Phys. Rev.* E **69** 046208
[32] Volya A and Zelevinsky V 2003 Non-hermitian effective hamiltonian and continuum shell model *Phys. Rev.* C **67** 054322
[33] Bulgakov E N and Sadreev A F 2011 Formation of bound states in the continuum for a quantum dot with variable width *Phys. Rev.* B **83** 235321